http://ansinet.com/itj

ITJ

ISSN 1812-5638

INFORMATION TECHNOLOGY JOURNAL

ANSInet
Asian Network for Scientific Information
308 Lasani Town, Sargodha Road, Faisalabad - Pakistan

Information Technology Journal 12 (6): 1168-1175, 2013
ISSN 1812-5638 / DOI: 10.3923/itj.2013.1168.1175

Single Image Dehazing Algorithm Based on Sky Region Segmentation

Gangyi Wang, Guanghui Ren, Lihui Jiang and Taifan Quan
School of Electronics and Information Technology, Harbin Institute of Technology,
Harbin, Heilongjiang, China

Abstract: Great progress has been made in image dehazing recently, while the sky region processed by these algorithms tends to be degraded by serious noise and color distortion. Based on the in-depth analysis on the degradation, the paper proposes an improved dehazing algorithm which first segments the haze image into the sky and non-sky region, then estimates the coefficients of the two regions separately, followed by the combination of the regions with a refining step. Experiment results show that the proposed algorithm provides significant advantage in generating smoother and more natural sky region, while keeping the non-sky region almost the same as the state of the art algorithms.

Key words: Image processing, dehazing, dark channel prior, sky region segmentation

INTRODUCTION

Dehazing for outdoor images serves as a key role in image processing and computer vision applications. The existence of haze reduces the quality of many image processing algorithms which assume input images captured in clear days. Therefore, dehazing becomes a necessary pre-processing module (Guo *et al*., 2012; Shuchun *et al*., 2011).

Many dehazing algorithms have been proposed based on different additional conditions. Some algorithms (Schechner *et al*., 2001; Narasimhan and Nayar, 2003a) require multiple images of the same scene with different degrees of polarization. Others use depth information which is obtained from multiple images (Hautiere *et al*., 2007) or manually specified by an expert (Narasimhan and Nayar, 2003b). Though algorithms based on multiple images could often get good results, their acquisitions are often constrained, while algorithms based on manually specified depth information could not work independently. Some algorithms (Chen *et al*., 2008) use the retinex theory to enhance the contrast of haze images, but the results have so far fallen short of expectations.

In recent years, significant progresses have been made in several dehazing algorithms (Fattal, 2008; Tan, 2008; He *et al*., 2009) based on the formation model of haze images. Without requiring multiple images or depth information, these algorithms can get really good results. The formation model of haze images used in these algorithms is shown as follows:

$$I(x) = J(x)t(x)+A(1-t(x)) \quad (1)$$

where x denotes a pixel in the scene, I(x) is the observed intensity at x, J(x) is the radiance at x, t(x) is the medium transmission from x to camera and A is the global atmospheric light. The task of a dehazing algorithm is to estimate t(x) and A from input I(x), then get J(x), which is the restored haze-free image.

In Eq. 1, the observed intensity I(x) consists of two terms: J(x)t(x) is called direct attenuation (Tan, 2008), representing the remaining intensity of scene radiance through the medium; A(1-t(x)) is called airlight, representing the scattered light from atmosphere. The transmission t(x) can be expressed as:

$$t(x) = e^{-\beta d(x)} \quad (2)$$

where, β is the medium scattering coefficient, d(x) is the distance from x to camera. In clear days, when practically no particle exists in the atmosphere, β is nearly zero, thus t(x) approaches 1, which means scene radiance j(x) could reach camera without being attenuated, while airlight A(1-t(x)) is 0, so we have j(x) equals to I(x). When the atmosphere particles get denser, β increases, t(x) decreases and more airlight mixes with scene radiance, so the blurred effect of haze images appears.

Equation 1 is applicable only to gray-scale images and in the case of color images, Eq. 3 replaces Eq. 1:

$$I^c(x) = J^c(x)t(x)+A^c(I-t)) \quad (3)$$

where, $c \in \{r, g, b\}$ is color channel index.

Fattal (2008) assume that the transmission and surface shading are locally uncorrelated and gets

Corresponding Author: Guanghui Ren, Harbin Institute of Technology, 342#, Harbin, Heilongjiang 150001, China
Tel/Fax: 86-451-86403135

good restoration result for images with light haze, but the algorithm cannot deal with images with dense haze. In Tan (2008) mades the estimates of the transmission t(x) by maximizing the local image contrast and refining t(x) with a MRF (Markov Random Field) model, but the restoration results are sometimes too saturated. He *et al*. (2009), proposes the dark channel prior, which is based on the assumption that most of the local regions in outdoor images have very low intensity in at least one color channel. With this prior, transmission can be effectively estimated. The haze-free images restored by this algorithm look more natural and the algorithm proves effective even for images with dense haze.

However, there is a common defect with the algorithms proposed by Tan (2008) and He *et al*. (2009) and in some other algorithms (Tarel and Hautiere, 2009): The restored images tend to accompany serious noise and color distortion in sky regions. To address this issue, we propose an improved dehazing algorithm, based on the dark channel prior algorithm, by segmenting the sky region of a haze image and estimating the transmission of the sky region and non-sky region separately. The proposed algorithm provides smoother and more natural sky region outputs. Furthermore, with the sky region segmented, the proposed algorithm can estimate the global atmospheric light A more accurately, which makes the restoration results more natural.

ANALYSIS OF THE NOISE AND COLOR DISTORTION OF THE SKY REGION

It is common to contain sky regions in outdoor images. The quality of the restored sky regions is very important to a dehazing algorithm. Figure 1 shows a restoration result generated by the dark channel prior algorithm.

The result shows that the non-sky region is restored quite well with the dark channel prior algorithm, but the sky region appears serious noise and color distortion. To explain this phenomenon, we can rewrite Eq. 1 as follows:

$$t(x)\bullet [A-J(x)] = A-I(x) \quad (4)$$

where, the term A-I(x) and A-J(x) are the intensity distances between x and the global atmospheric light A in haze and haze-free images respectively. Therefore, the process of adding haze to a pixel x can be understood as reducing the intensity distance between x and the global atmospheric light A by the ratio of t(x), as is shown in Fig. 2.

As the intensity distance is reduced between A and every pixel in the haze image, the contrast of the haze image is also reduced and the intensity of the whole image is increased. The process of removing haze is equivalent to a contrast enhancement process, whose enhancement ratio is controlled by t(x), which is to be estimated from the haze image. Many dehazing algorithms based on Eq. 1, including the "dark channel prior" algorithm, are intended to increase the contrast of the haze image as much as possible under certain constraints. In the non-sky region, this strategy makes the restored image clearer. While in the sky region, intensity is distributed randomly in a small range near the atmospheric light A. Enhancing the contrast of the sky region as much as possible makes the intensity distributed randomly in a much wider range, which leaves the sky region accompanied with serious

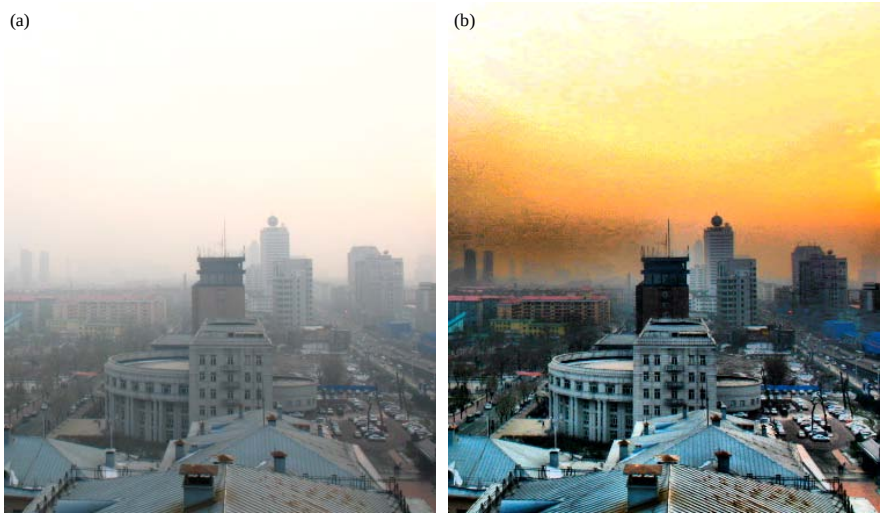

Fig. 1(a-b): Restoration result by dark channel prior. (a) Haze image and (b) Restored image

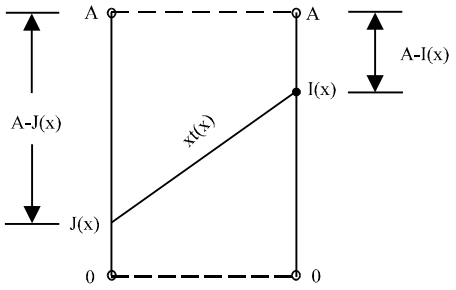

Fig. 2: The process of adding haze to a pixel x

noise and color distortion. To address this issue, Yan in (Wang and Wu, 2010) restricts t(x) to be no smaller than 0.3. In this way, the sky region would not be enhanced too much. However, for regions with dense haze, t(x) is usually much smaller than 0.3, restricting t(x) above 0.3 leads to the contrast enhancement in such regions insufficient.

PROPOSED ALGORITHM

Different strategies should be employed to estimate t(x). The contrast in the non-sky region should be enhanced as much as possible, while the enhancement ratio in the sky region should be properly reduced. Based on this strategy, the proposed algorithm is shown in Fig. 3.

The haze image is first segmented into the sky region and the non-sky region, followed by the estimation of the global atmospheric light A with the sky region. After that, t(x) in the sky region and non-sky region is estimated separately. Then the two parts of t(x) are merged and refined and finally the scene radiance J(x) is restored, which is the haze-free image. The modules are to be discussed one by one in the following sections.

Segmenting the sky region: In outdoor images, the sky is usually a large and smooth region with high intensity. Based on this feature, we can first find out all the smooth and bright connected regions, then select the region with the largest area and mark it as the sky region. The detailed steps are listed below:

Step 1: Compute the gradient of each pixel in the input image to get a gradient image D(x)

Step 2: Transform D(x) into a binary image $B_1(x)$, whose value is '1' if D(x) is smaller than threshold θ, otherwise is '0'

Step 3: Erode $B_1(x)$ with a square template of radius r to get a binary image $B_2(x)$

Step 4: Get all the connected regions with region growing algorithm in the binary image $B_2(x)$ and pick out the connected regions whose average intensity is larger than threshold T

Step 5: Select the connected region with the largest area as the sky region

In step 2, θ is the threshold to determining whether a pixel is in a smooth region, thus, binary image $B_1(x)$ labels all the smooth pixels in the input image. The erosion operation on $B_1(x)$ prevents the sky region from connecting to the non-sky region along a narrow path on which intensity changes slowly. The connected regions whose average intensity is smaller than threshold T is discarded, thus preventing dark connected regions from being determined as the sky region. Figure 4a shows the segmentation result, in which pixels in the sky region are labeled with gray color. Parameters used here are $\theta = 0.02$, $r = 3$, $T = 0.81_{max}$, where, I_{max} denotes the highest intensity in the input image.

Two defects are spotted in the segmented sky region in Fig. 4a. One is the boundary of the sky region is rough, which is mainly caused by the erosion operation of step 3, the other is the existence of small holes in the sky region, the consequence of noise pixels. So two more steps are needed:

Step 6: Search for the pixels in the non-sky region whose space distances to the sky region are smaller than r and intensity distances are smaller than θ, then add these pixels into the sky region

Step 7: Fill the holes to add the noise pixels into the sky region

Figure 4b shows the final refined sky region. The segmentation result may be not very precise, but is enough for the following modules.

Estimating the global atmospheric light: The global atmospheric light A needs to be estimated before t(x). Although, A is a constant parameter within the whole image, yet its precision can greatly affects the final restoration result. A common approach (Tan, 2008) is to use the pixel with highest intensity in the input image as A. But in images containing other light sources such as lamps, the highest intensity could be greater than A.

As the sky region has been segmented previously, A can be estimated as the average intensity (average RGB values for color images) of the sky region. It's simple but effective, because pixels in the sky region can be

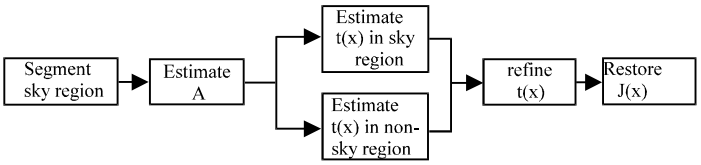

Fig. 3: Flow diagram of the proposed algorithm

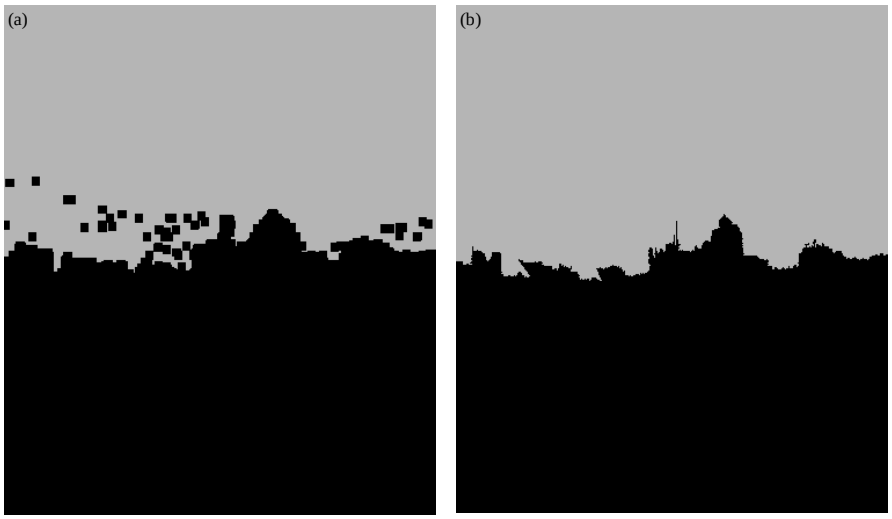

Fig. 4(a-b): Segmented sky region, (a) Roughly segmented sky region and (b) Refined sky region

considered as infinity, which means t(x) = 0 and I(x) = A in these pixels, according to Eq. 1 and Eq. 2. Therefore, the average intensity of the sky region is an ideal estimation of A.

Estimating the medium transmission: The next step is the estimation of the medium transmission t(x). In Eq. 2, t(x) relates to the distance d(x) between scene and camera. However, it's not easy to estimate d(x) from a single image; meanwhile, the other parameter β in Eq. 2 is also hard to estimate. Thus, it's more practical to estimate t(x) directly, without using Eq. 2.

The dark channel prior algorithm (He *et al*., 2009) is a simple but effective way to estimate t(x), we employ it in our algorithm. The dark channel prior assumes that in most of the non-sky patches, at least one color channel has very low intensity at some pixels (He *et al*., 2009). For va haze-free image J(x), define:

$$J^{dark}(x) = \min_{c\in\{r,g,b\}} \left(\min_{y\in\Omega(x)} (J^c(y)) \right) \quad (5)$$

where, Ω(x) is a local patch centered at x, J^{dark} (x), is referred as the dark channel of J(x). The dark channel of each pixel in a haze-free image tends to be zero except in the sky region. The prior is verified by He *et al.* (2009) to be true in most haze-free images.

In haze images, due to the addictive airlight, the intensity of dark channel is no longer near-zero. With the assumption that pixels in the local patch centered at x has the same transmission $\tilde{t}$, taking the min operation on Eq. 5, we have:

$$\min_{y\in\Omega(x)} (I^c(y)) = \tilde{t}(x) \min_{y\in\Omega(x)} (J^c(y)) + (1-\tilde{t}(x))A^c \quad (6)$$

Divide Eq. 6 with A^c and take the min operation among three color channels to get the following equation:

$$\min_c \left(\min_{y\in\Omega(x)} \left(\frac{I^c(y)}{A^c} \right) \right) = \tilde{t}(x) \min_c \left(\min_{y\in\Omega(x)} \left(\frac{(J^c(y))}{A^c} \right) \right) + (1-\tilde{t}(x)) \quad (7)$$

According to the dark channel prior, we have:

$$\min_{c\in\{r,g,b\}} \left(\min_{y\in\Omega(x)} (J^c(y)) \right) = J^{dark}(x) = 0 \quad (8)$$

Putting Eq. 8 into Eq. 7, we can get the estimation of t(x) as the following equation:

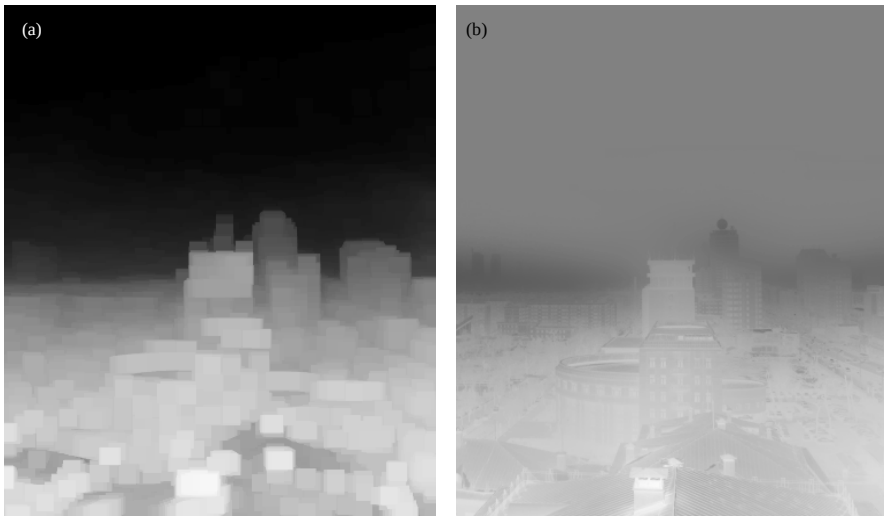

Fig. 5(a-b): Estimated t(x), (a) Roughly estimated t(x), (b) Refined t(x) with guilded filter

$$\tilde{t}(x)=1-\min_{c}\left(\min_{y\in\Omega(x)}\left(\frac{I^{c}(y)}{A^{c}}\right)\right) \quad (9)$$

Figure 5a is the estimated t(x) of the haze image in Fig. 1a.

As the dark channel prior is not true for the sky region, estimate t(x) in the sky region with dark channel prior would get restoration result like Fig. 1b. Therefore, we simply set all the t(x) in the sky region with a constant t_{sky}.

Refining the medium transmission: It can be seen from Fig. 5a that the estimation of t(x) with the dark channel prior is rough, which usually introduces halos into the final restoration result, so an algorithm to refine t(x) is needed. Many existing algorithms can be used, such as soft matting (He *et al*., 2010), MRF based methods, joint bilateral filtering (Petschnigg *et al*., 2004), guided filtering (He *et al*., 2010), etc. The guided filtering algorithm is chosen here for its relatively high refining quality and low time-consumption.

The guided filtering algorithm uses the haze image as a guide to refine the estimated t(x) image, whose process is essentially an edge preserving filtering. For detailed information about guided filtering, refer to (He *et al*., 2010).

Ast(x) is estimated separately in the sky region and non-sky region, t(x) of the two regions are combined before the refining step so that the boundary of the two regions in the final restoration image looks smoother than the case of combination after the refining step. Figure 5b shows the refined image of t(x).

Restoring the scene radiance: After the estimation of A and t(x), we can rewrite Eq. 3 as follows:

$$J^{c}(x)=A^{c}-\frac{A^{c}-I^{c}(x)}{t(x)} \quad (10)$$

With Eq. 10, we can directly get the scene radiance J(x). Fig. 6(a) shows the J(x) image.

The restored image in Fig. 6(a) looks dim, which is usually caused by the airlight in the haze image that makes the exposure of the camera insufficient. To solve this problem, the J(x) image is enhanced through the following steps:

Step1: Transform J(x) to HSV (Hue, Saturation and Value) color space

Step2: Enhance the contrast of the V component with CLAHE (Contrast Limited Adaptive Histogram Equalization) algorithm

Step3: Transform the enhanced HSV image back to RGB color space to get the final restoration result.

Figure 6b shows the image enhanced with the method above, in which brightness and the contrast are greatly enhanced compared with Fig. 6a.

RESULTS AND DISCUSSION

In order to test the effect of the proposed algorithm, we compare our algorithm with the original dark channel prior algorithm in Fig. 7. The parameters used in our algorithm for Fig. 7 are $\theta = 0.02$, $r = 3$, $T = 0.81_{max}$.

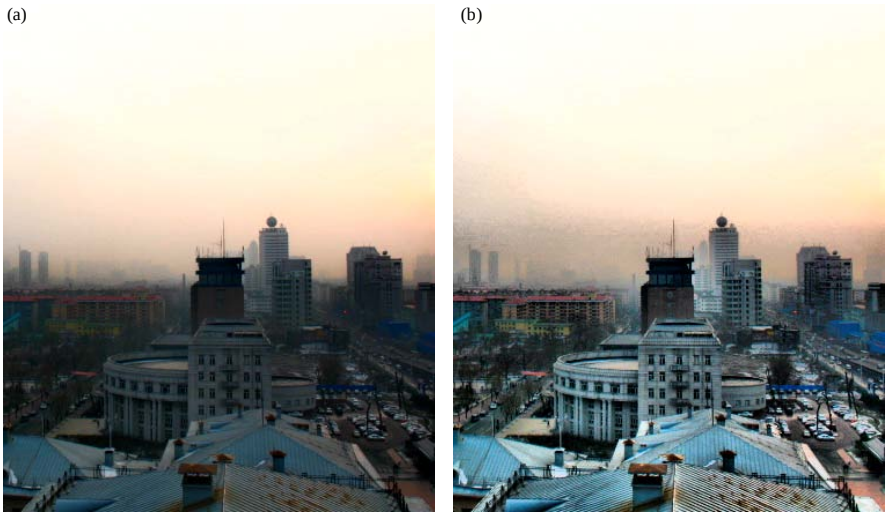

Fig. 6(a-b): Restoration result, (a) Restored image J(x) and (b) Final result after enhancement

Fig. 7(a-f): Comparison of our algorithm and the original dark channel prior algorithm. Left column: haze images. Middle column: result by the original dark channel prior algorithm. Right column: result by the proposed algorithm

Fig. 8(a-b): Restoration result for an image with no sky region, (a) Haze image and (b) Restored image

Table 1: Entropies in the sky regions (bits/pixel)

Original image	Entropy/restored image by dark channel prior	Entropy/restored image by proposed algorithm
Fig. 1a	6.685/Fig. 1b	3.740/Fig. 6b
Fig. 7a	6.497/Fig. 7b	4.323/Fig. 7c
Fig. 7d	6.723/Fig. 7e	4.673/Fig. 7f

The results of comparison show that the sky region processed by our algorithm looks smoother and more natural. In order to evaluate the improvement quantitatively, we compute the entropies of the sky regions generated by the two algorithms, as shown in Table 1. Theoretically, the entropy of the sky region should be nearly zero, because there is hardly information in the sky region. As listed in Table 1, our algorithm gives lower entropies than the dark channel prior algorithm does, which indicates that our algorithm generates more natural sky regions.

However, the quality of the restoration result in the regions near the sky region declines slightly, which is because t(x) in these regions is influenced by the sky region during the refining step. Figure 8 shows a failure example by our algorithm. As there is no sky region in the haze image, our algorithm incorrectly selects a region whose haze is densest (region surrounded by red line) as the sky region, which makes the restoration result decline in this region. Therefore, our algorithm is only suitable with the images which contain sky region.

CONCLUSION

In this study, we propose an improved dehazing algorithm, which segments a haze image into sky and non-sky regions and estimates the medium transmission of the two regions separately. Based on this algorithm, the restoration result of the sky region is significantly improved, which is smoother and more natural than most other dehazing algorithms. Furthermore, with the segmentation of the sky region, the global atmospheric light can be estimated more precisely. The experiment results show that the algorithm is effective. But there are still a couple of drawbacks for the algorithm as follows:

- For the images with no sky region, the algorithm selects dense-haze regions as the sky regions, the restoration results in these regions may decline
- Affected by the transmission refining step, restoration results in the regions near the sky region may be influenced by the sky region

For the limitations above, we intend to develop algorithms to detect sky region and combine the sky region and non-sky region more smoothly.

REFERENCES

Chen, X., X. Yan and X. Chu, 2008. Fast algorithms for foggy image enhancement based on convolution. Proceedings of the International Symposium on Computational Intelligence and Design, Volume 2, October 17-18, 2008, Wuhan, China, pp: 165-168.

Fattal, R., 2008. Single image dehazing. ACM Trans. Graphics, Vol. 27, No. 3.

Guo, F., Z. Cai, B. Xie and J. Tang, 2012. Review and prospect of image dehazing techniques. J. Comput. Appli., 30: 2417-2421.

Hautiere, N., J.P. Tarel and D. Aubert, 2007. Towards fog-free in-vehicle vision systems through contrast restoration. Proceedings of the IEEE Conference on Computer Vision and Pattern Recognition, June 17-22, 2007, Minneapolis, MN., USA., pp: 1-8.

He, K., J. Sun and X. Tang, 2009. Single image haze removal using dark channel prior. Proceedings of the IEEE Conference on Computer Vision and Pattern Recognition, June 20-25, 2009, Miami, FL., USA., pp: 1956-1963.

He, K., J. Sun and X. Tang, 2010. Guided image filtering. Proceedings of the 11th European Conference on Computer Vision: Part I, September 5-11, 2010, Heraklion, Crete, Greece, pp: 1-14.

Narasimhan, S.G. and S.K. Nayar, 2003a. Contrast restoration of weather degraded images. IEEE Trans. Pattern Anal. Mach. Intell., 25: 713-724.

Narasimhan, S.G. and S.K. Nayar, 2003b. Interactive (De) weathering of an image using physical models. Proceedings of the IEEE Workshop on Color and Photometric Methods in Computer Vision, October 11-17, 2003, Nice, France, pp: 1-8.

Petschnigg, G., R. Szeliski, M. Agrawala, M. Cohen, H. Hoppe and K. Toyama, 2004. Digital photography with flash and no-flash image pairs. ACM Trans. Graphics, 23: 664-672.

Schechner, Y.Y., S.G. Narasimhan and S.K. Nayar, 2001. Instant dehazing of images using polarization. Proceedings of the IEEE Computer Society Conference on Computer Vision and Pattern Recognition, Volume 1, December 8-14, 2001, Kauai, HI., USA., pp: 325-332.

Shuchun, Y., Y. Xiaoyang, S. lina, Z. Yuping and S. Yongbin et al., 2011. A reconstruction method for disparity image based on region segmentation and RBF neural network. Inform. Technol. J., 10: 1050-1055.

Tan, R.T., 2008. Visibility in bad weather from a single image. Proceedings of the IEEE Conference on Computer Vision and Pattern Recognition, June 23-28, 2008, Anchorage, AK., USA., pp: 1-8.

Tarel, J.P. and N. Hautiere, 2009. Fast visibility restoration from a single color or gray level image. Proceedings of the IEEE 12th International Conference on Computer Vision, September 29-October 2, 2009, Kyoto, Japan, pp: 2201-2208.

Wang, Y. and B. Wu, 2010. Improved single image dehazing using dark channel prior. Proceedings of the IEEE International Conference on Intelligent Computing and Intelligent Systems, Volume 2, October 29-31, 2010, Xiamen, China, pp: 789-792.